

Syntheses, Structures and Reactivities of Rhodium 4,5-Diazafluorene Derivatives

Huiling Jiang,^[a] Elzbieta Stepowska,^[a] and Datong Song*^[a]

Keywords: Heterocycles / Rhodium / Hydrogenation / Alkenes

Four rhodium 4,5-diazafluorene derivatives, $[\text{RhL}(\text{PPh}_3)_2]$ (**1**), $[\text{Rh}(\text{H})_2(\text{LH})(\text{PPh}_3)_2]\text{Cl}$ (**2**), $[\text{Rh}(\text{H})_2\text{L}(\text{PPh}_3)_2]$ (**3**) and $[\text{Rh}(\text{H})_2(\text{LH})(\text{PPh}_3)_2]\text{OTf}$ (**4**), have been synthesized and fully characterized by NMR spectroscopy, elemental analysis and single-crystal X-ray diffraction. Compound **1** can be converted into **3** when treated with hydrogen gas. Compound **2** can be converted into **3** when treated with NaH, and the reverse reaction can be achieved by treating **3** with aqueous HCl. The

air- and moisture-stable compound **2** is an active catalyst for the hydrogenation of a variety of olefins, including non-terminal ones; the chloride counterion in **2** appears to play a role in the catalytic system. Thus, compound **4**, the triflate analogue of **2**, is inactive towards olefin hydrogenation.

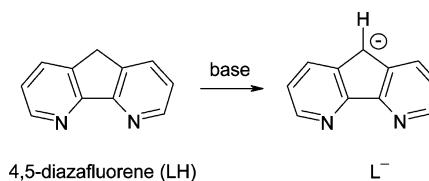
(© Wiley-VCH Verlag GmbH & Co. KGaA, 69451 Weinheim, Germany, 2009)

Introduction

Although 4,5-diazafluorene (LH) was first reported over three decades ago,^[1] its coordination chemistry is largely unexplored.^[1–3] The most studied coordination compounds of LH are the Ru complexes because of their potential application in photochemical water-splitting processes.^[2] In these cases, the LH ligand was viewed as a 3,3'-annealed bipyridine. Previously our group discovered the facile aerobic oxidation of the $\text{C}(\text{sp}^3)\text{--H}$ bonds of *cis,cis,cis*- $[\text{RuCl}_2(\text{LH})(\text{PPh}_3)_2]$ in which the CH_2 group of the LH ligand is oxidized to a carbonyl group by air leaving the phosphane ligands intact.^[4]

The structure of LH can be viewed as two pyridine rings fused onto a cyclopentadiene (CpH) ring in a *syn* fashion. Therefore, it is conceivable that if LH is deprotonated at the 9-position, the resulting 4,5-diazafluorenyl (L^-) has two types of metal-binding sites, the pyridine nitrogen donors and the C^- carbon donor (Scheme 1), that can potentially accommodate two different metal centres. In addition, the L^- ligand is able to form zwitterionic complexes^[5] when only the two nitrogen donor atoms are involved in the binding of metal ions owing to the -1 charge on the ligand backbone. Despite such interesting structural features displayed by L^- , metal complexes of the L^- ligand are barely known.^[5]

In our previous report^[5] we described the coordination chemistry of L^- with Na^+ , Pd^{II} and Rh^{I} , as well as the catalytic activity of $[\text{RhL}(\text{cod})]$ towards olefin hydrogenation. Unlike Wilkinson's catalyst, $[\text{RhCl}(\text{PPh}_3)_3]$, which is thermally unstable and undergoes ligand dissociation in solu-



Scheme 1. Conversion of LH to L^- .

tion, $[\text{RhL}(\text{cod})]$ is thermally stable in solution. Similar to Wilkinson's catalyst, $[\text{RhL}(\text{cod})]$ is air-sensitive in solution, however, it is not as active as Wilkinson's catalyst for olefin hydrogenation. Our previous study indicated that $[\text{RhL}(\text{cod})]$ does not promote the hydrogenation of non-terminal $\text{C}=\text{C}$ double bonds. Furthermore, the cod ligand appeared to bind to the metal centre strongly, which might be responsible for the low activity of $[\text{RhL}(\text{cod})]$ in olefin hydrogenation. The $[\text{RhL}(\text{cod})]$ complex is the first reported Rh complex of the L^- ligand. To the best of our knowledge, Rh complexes of the charge-neutral LH ligand are still unknown.

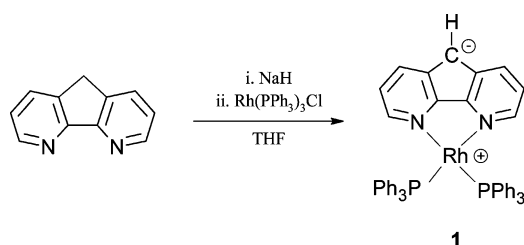
To expand the coordination chemistry of the LH and L^- ligands, we recently prepared a series of Rh complexes of both LH and L^- ligands bearing triphenylphosphane as the neutral ancillary ligand. These include the first Rh complexes of the charge-neutral LH ligand. Under appropriate conditions these complexes can interconvert. One of the resulting complexes, $[\text{Rh}(\text{H})_2(\text{LH})(\text{PPh}_3)_2]\text{Cl}$ (**2**) shows unique catalytic reactivity towards olefin hydrogenation. The chloride counterion appears to play a role in olefin hydrogenation reactions catalysed by **2**. The syntheses, structures, spectroscopic data and reactivities of these compounds are reported herein.

[a] Davenport Chemical Research Laboratories, Department of Chemistry, University of Toronto, 80 St. George Street, Toronto, Ontario, M5S 3H6, Canada
Fax: +1-416-978-7013
E-mail: dsong@chem.utoronto.ca

Results and Discussion

Synthesis and Structure of $[\text{RhL}(\text{PPh}_3)_2]$ (**1**)

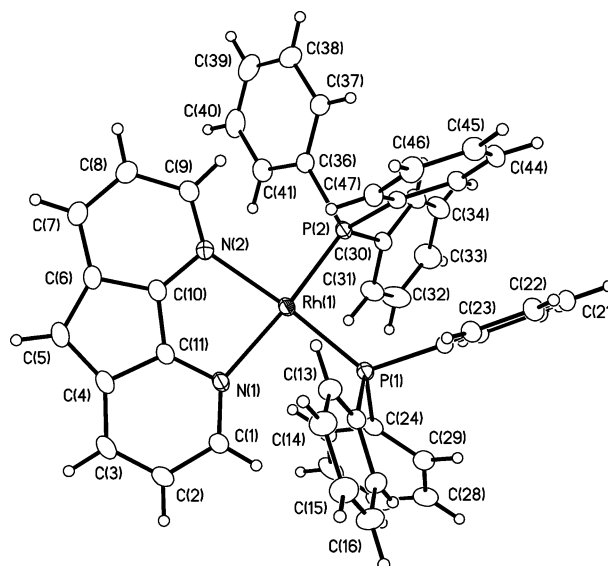
The reaction of in situ generated NaL and $[\text{RhCl}(\text{PPh}_3)_3]$ gave **1** in 76% yield (Scheme 2). NMR experiments indicated that this reaction is incomplete, that is, a small amount of $[\text{RhCl}(\text{PPh}_3)_3]$ and its decomposition products are always present. These impurities can be removed by recrystallization to generate analytically pure compound **1**. The dark-green compound **1** is soluble in most common organic solvents, except for the non-polar hexanes and pentane. It is air-stable in the solid state, but air-sensitive in solution. Unlike $[\text{RhCl}(\text{PPh}_3)_3]$, which is thermally unstable in solution at ambient temperature, compound **1** is thermally stable in both the solid state and in solution at ambient temperature.

Scheme 2. Synthesis of **1**.

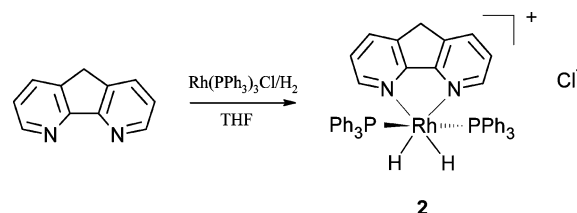
The proton of the Cp ring of the L^- ligand in **1** resonates at $\delta = 6.53$ ppm as a singlet in the ^1H NMR spectrum in C_6D_6 , upfield-shifted relative to its counterpart in $[\text{RhL}(\text{cod})]$ ($\delta = 6.72$ ppm),^[5] which can be attributed to the stronger σ -donating and weaker π -accepting abilities of the phosphane ligands compared with the cod ligand. The same trend was observed with the remaining proton signals of the L^- ligand. The ^{31}P NMR spectrum of compound **1** exhibits one doublet signal at $\delta = 52.11$ ppm with a $^1J_{\text{P-Rh}}$ coupling constant of 187 Hz, which is in the reported range for one-bond $^{31}\text{P}-^{103}\text{Rh}$ coupling.^[6]

The molecular structure of **1** in the solid state was confirmed by X-ray crystallography. As shown in Figure 1, the Rh^{I} centre adopts a distorted square-planar coordination geometry with the two nitrogen donor atoms of the L^- ligand and the two phosphorus donor atoms of the two triphenylphosphane ligands occupying the four coordination sites. Because of the repulsion between the two phosphane ligands, the two phosphorus donor atoms P(1) and P(2) reside on different sides of the plane defined by the five-membered chelate ring with distances to the plane of approximately 0.35 and 0.51 Å, respectively. The bite angle of the L^- ligand is $82.10(9)^\circ$. The L^- ligand is slightly bent rather than planar, presumably because of the repulsion between L^- and the phosphane ligands. The C(4)–C(5) and C(5)–C(6) bond lengths are 1.412(5) and 1.419(4) Å, respectively, close to typical aromatic C–C bond lengths. The C(4)–C(5)–C(6) angle is $107.7(3)^\circ$, similar to that observed for the L^- ligand in $[\text{Na}_2\text{L}_2(\text{LH})_2]$ and $[\text{RhL}(\text{cod})]$.^[5] The Rh–N bonds [2.196(2) and 2.199(2) Å] in compound **1** are longer than those in $[\text{RhL}(\text{cod})]$ [both 2.147(2) Å] as a result of the

bulkiness and the *trans* effect of the phosphane ligands. Two phenyl rings from the two phosphane ligands interact with each other with a contact distance of around 3.2 Å.

Figure 1. Molecular structure of **1** with thermal ellipsoids plotted at the 30% probability level.Synthesis and Structure of $[\text{Rh}(\text{LH})(\text{PPh}_3)_2(\text{H})_2]\text{Cl}$ (**2**)

The neutral LH ligand and $[\text{Rh}(\text{PPh}_3)_3\text{Cl}]$ gave no observable reaction in THF under argon. When hydrogen was introduced to replace argon, compound **2** could be isolated as a pale-pink precipitate in quantitative yield within an hour (Scheme 3). Compound **2** is insoluble in THF and benzene, but soluble in alcohol and chlorinated solvents such as CH_2Cl_2 and CHCl_3 . Unlike compound **1**, compound **2** is air- and moisture-stable in both the solid state and solution. The CH_2 group of the LH ligand in compound **2** displays a singlet at $\delta = 3.83$ ppm in the ^1H NMR spectrum in CD_2Cl_2 . The doublet of triplets at $\delta = -16.8$ ppm, integrated to 2 H, originates from the two hydride atoms coupled to one Rh and two P nuclei with $^1J_{\text{Rh-H}}$ and $^2J_{\text{P-H}}$ values of 18 and 13 Hz, respectively. The ^{31}P NMR spectrum of **2** exhibits a doublet of triplets at $\delta = 48.62$ ppm with $^1J_{\text{Rh-P}}$ and $^2J_{\text{P-H}}$ values of 116 and 11 Hz, respectively. The $^{31}\text{P}-^{103}\text{Rh}$ coupling constant is smaller than that in **1** and similar to the literature value for $[\text{Rh}(\text{H})_2(\text{phen})(\text{PPh}_3)_2][\text{SB}_9\text{H}_{12}]$.^[7]

Scheme 3. Synthesis of **2**.

The structure of **2** in the solid state was established by X-ray crystallography and the cationic portion is shown in Figure 2. The Rh^{III} centre adopts a distorted octahedral coordination geometry with the two hydrides, the two nitrogen donor atoms of the LH ligand and the two phosphorus donor atoms of the two triphenylphosphane ligands occupying the six coordination sites. The two hydrides are *cis* to each other, whereas the two phosphane ligands are *trans* to each other, consistent with the solution NMR spectroscopic data. A crystallographically imposed mirror plane slices through the LH ligand, the Rh centre, the two hydrides and the chloride counterion. Therefore the two phosphane ligands are mirror images of each other. The Rh(1)–N(1) and Rh(1)–N(2) bond lengths are 2.234(3) and 2.223(3) Å, respectively, longer than those in compound **1**. This could be attributed to the strong *trans* effect of the hydride ligands in **2**. The Rh–P bonds in **2** [2.2994(8) Å] are longer than those in **1** [2.2217(7) and 2.2357(7) Å] because of the *trans* arrangement of the two phosphane ligands in **2**, which weakens the Rh–P bonds. This is consistent with the smaller ³¹P–¹⁰³Rh coupling constant in the ³¹P NMR spectrum. The P(1)–Rh–P(1A) angle is 170.60(4)°, smaller than the ideal 180° for a regular octahedron because of the repulsion between the bulky phosphane and LH ligands. The C(4)–C(5) and C(5)–C(6) bond lengths are 1.513(6) and 1.532(6) Å, respectively, typical of C–C single bonds. The C(4)–C(5)–C(6) angle of the LH ligand in **2** is 101.8(3)°, similar to that observed for the LH ligand in [Na₂(LH)₂L₂].^[5] The bite angle of the chelating ligand in **2** is 80.53(12)°, slightly smaller than that in **1**.

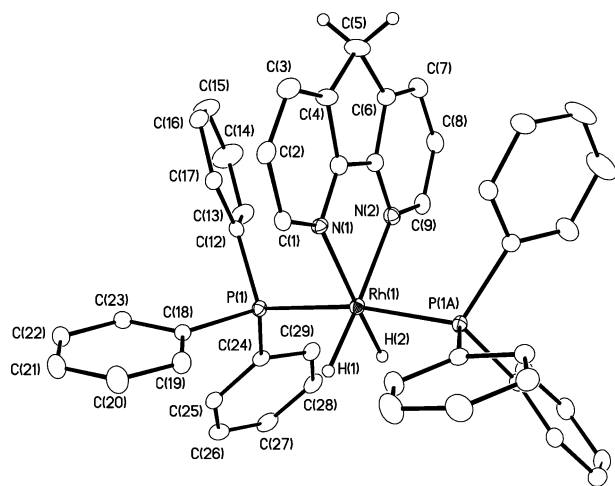
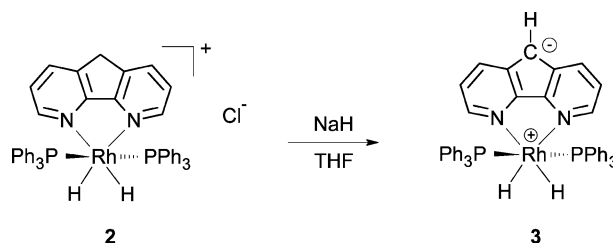


Figure 2. Molecular structure of the Rh-containing cation of **2** with thermal ellipsoids plotted at the 30% probability level. The chloride counterion and most of the hydrogen atoms have been omitted for clarity.

Synthesis and Structure of [Rh(PPh₃)₂H₂L] (**3**)

Compound **3** can be prepared in quantitative yield by treating **2** with NaH (Scheme 4). In the ¹H NMR spectrum of **3**, the proton at the 9-position of the chelating ligand resonates at $\delta = 6.29$ ppm, which indicates the aromaticity

of the central C₅ ring of the L[−] ligand in **3**. A doublet of triplets at -16.49 ppm originates from the two hydrides coupled to one rhodium and two phosphorus nuclei with coupling constants of 17 and 15 Hz, respectively. The ³¹P NMR spectrum of **3** exhibits a doublet of triplets at $\delta = 50.19$ ppm with ¹J_{Rh–P} and ²J_{H–P} values of 118 and 10 Hz, respectively. All the coupling constants are similar to those displayed by **2**.



Scheme 4. Synthesis of **3**.

The molecular structure of compound **3** in the solid state was confirmed by single-crystal X-ray diffraction analysis. As shown in Figure 3, the Rh^{III} centre adopts a distorted octahedral coordination geometry with the two nitrogen donor atoms of the L[−] ligand, the two hydrides and the two phosphorus donor atoms of the two triphenylphosphane ligands occupying the six coordination sites in a *cis,cis,trans* fashion. The C(4)–C(5) and C(5)–C(6) bond lengths are 1.403(8) and 1.426(8) Å, respectively, typical of aromatic C–C bonds. The C(4)–C(5)–C(6) angle is 108.6(5)°, close to the ideal angle for a regular pentagon. The repulsion between L[−] and the two bulky phosphane ligands pushes the two phosphane ligands away from the L[−] ligand and thus the P(1)–Rh(1)–P(2) angle is 162.85(5)°, smaller than the ideal 180° for a regular octahedron. This distortion is more significant than that in **2**.

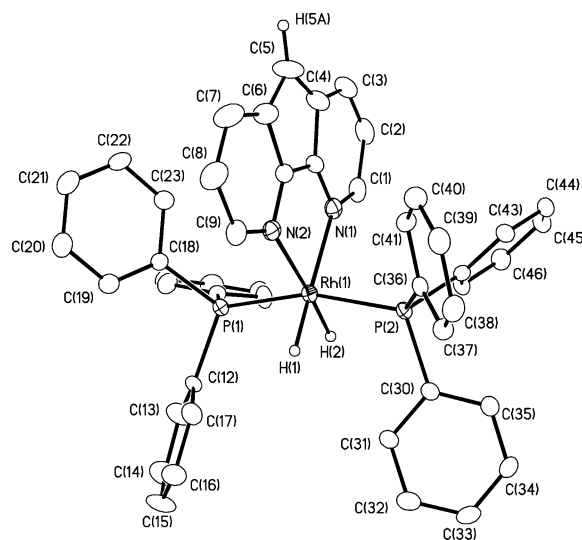
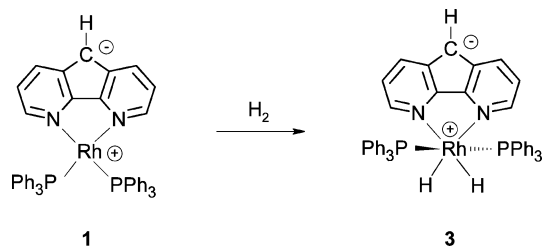


Figure 3. Molecular structure of **3** with thermal ellipsoids plotted at the 30% probability level. All of the hydrogen atoms (except for the hydrides and the hydrogen atom of the Cp ring) have been omitted for clarity.

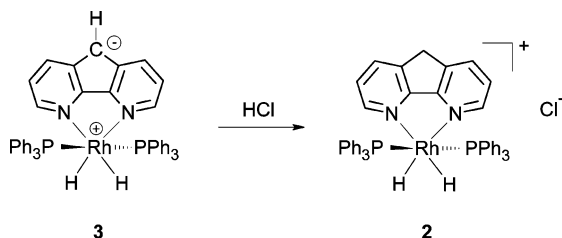
Reactivities of 1–3

When treated with 1 atm of H₂, compound **1** can be converted into compound **3** quantitatively (Scheme 5). Although this reaction is fast and clean, the synthesis of compound **3** by the reaction of **2** with NaH is a better route. The main reason for this is that the synthesis from **2** gives a quantitative yield and requires virtually no purification, whereas the synthesis from **1** gives a lower yield and requires recrystallization.

Scheme 5. Conversion of **1** into **3**.

Compound **3** reacts with styrene slowly to afford ethylbenzene and compound **1**. The slow reaction rate makes this conversion of no practical use. Thus, in the presence of a large excess of styrene it takes a month to achieve around 50% conversion from **3** to **1**. As expected, both **1** and **3** are poor catalysts for olefin hydrogenation. The unpurified compound **1** shows good activity towards olefin hydrogenation because of contamination by [RhCl(PPh₃)₃] and its decomposition products.

As described above, compound **3** can be obtained in quantitative yield by treating **2** with a strong base such as NaH. This conversion can be reversed cleanly by treating compound **3** with a 10% HCl aqueous solution. During this reaction the L[−] ligand in **3** is protonated at the 9-position to generate the LH ligand, leaving the hydrides on the rhodium centre intact (Scheme 6), even with an excess amount of HCl.

Scheme 6. Conversion of **3** into **2**.Olefin Hydrogenation Promoted by **2**

The air- and moisture-stable compound **2** is able to promote the hydrogenation of olefins under mild conditions with low catalyst loading. As shown in Table 1, not only simple terminal olefins (entries 1 and 2), but also terminal olefins with functional groups (entries 3–5) can be hydrogenated, leaving the polar C=O and C=N bonds intact. Unlike the previously reported [Rh(cod)L], which does not

promote the hydrogenation of internal olefins, compound **2** is able to promote the hydrogenation of non-terminal olefins (entries 6 and 7).

Table 1. Hydrogenation of olefins promoted by **2**.

Entry	Substrate ^[a]	Product ^[b]	Time (h) ^[c]	TOF ^[d] (h ^{−1})
1			6	333
2			27	74
3			4	500
4			64	31
5			8	250
6			12	167
7			30	67

[a] 7 M in MeOH, 0.05 mol-% of **2**, 1 atm of H₂, ambient temperature. [b] Products in entries 1,^[8] 2,^[9] 3,^[9] 4,^[10] 5,^[11] 6,^[12] and 7^[13] were identified by ¹H NMR spectroscopy. [c] Time required for 100% conversion, monitored by NMR spectroscopy. [d] Turnover frequency.

We also compared the relative efficiencies of [Rh(PPh₃)₃Cl], [Ru(PPh₃)₃Cl₂] and compound **2** in promoting the hydrogenation of styrene. Under otherwise identical conditions (i.e., ambient temperature, 1 atm of H₂, 7 M of styrene, 0.05 mol-% catalyst loading, MeOH, 8 h) the hydrogenation reactions catalysed by **2**, [Ru(PPh₃)₃Cl₂] and [Rh(PPh₃)₃Cl] gave 50, 77 and 100% conversions, respectively.

Our preliminary study indicated that hydrogen pressure does not affect the reaction rate of styrene hydrogenation in MeOH promoted by compound **2**. Thus, the reaction rates are comparable under 1 and 4 atm of H₂. In contrast, styrene hydrogenation in benzene promoted by [Rh(cod)L] is faster with higher hydrogen pressure. The addition of PPh₃ or LH ligand slows the hydrogenation process, which implies that ligand dissociation is crucial in the catalytic cycle. One hypothesis is that the chloride counterion exchanges with the LH ligand on the Rh centre to form Wilkinson's catalyst, which is the active catalyst in the system. Because LH is a chelating ligand, only a small amount of Wilkinson's catalyst exists in this equilibrium. If this was the case, at higher chloride concentrations the hydrogenation should be faster because the concentration of Wilkinson's catalyst in the system would increase. However, the addition of 1 equiv. of BuN₄Cl (relative to **2**) to the catalytic system slows the hydrogenation process slightly. This prompted us to synthesize the chloride-free version of compound **2**, expecting improvements in the olefin hydrogenation.

Synthesis and Structure of $[\text{Rh}(\text{H})_2(\text{LH})(\text{PPh}_3)_2]\text{OTf}$ (**4**)

Compound $[\text{Rh}(\text{H})_2(\text{LH})(\text{PPh}_3)_2]\text{OTf}$ (**4**) was synthesized in 84% yield by treating compound **2** with 1 equiv. of AgOTf . Similarly to **2**, compound **4** is colourless and air- and moisture-stable in both the solid state and solution. The crystal structure of **4** was confirmed by X-ray crystallography (Figure 4). Unlike that of **2**, the structure of **4** has no crystallographically imposed symmetry through the Rh-containing cation. The six phenyl groups of the two triphenylphosphane ligands are staggered along the P(1)–P(2) axis, whereas those in **2** are eclipsed as a result of the mirror-plane symmetry. Otherwise the structures of the cationic portions of **2** and **4** are similar to each another in terms of the metric parameters within the LH ligand and around the metal centre (see Table 2). The OTf^- counterions are located between the cationic portions, interacting with the cations through multiple hydrogen bonds. The ^1H NMR spectrum of **4** in CD_3OD exhibits a doublet of triplets at -16.75 ppm ($^1J_{\text{Rh-H}} = 18$ Hz, $^2J_{\text{P-H}} = 13$ Hz). The ^{31}P NMR spectrum of **4** shows a doublet of triplets at $\delta = 48.28$ ppm ($^1J_{\text{Rh-P}} = 116$ Hz, $^2J_{\text{P-H}} = 11$ Hz). To our surprise, **4** was inactive towards styrene hydrogenation, which indicates that the Cl^- counterion in **2** probably plays a role in the catalytic system. However, its role is not fully understood yet and will be investigated further.

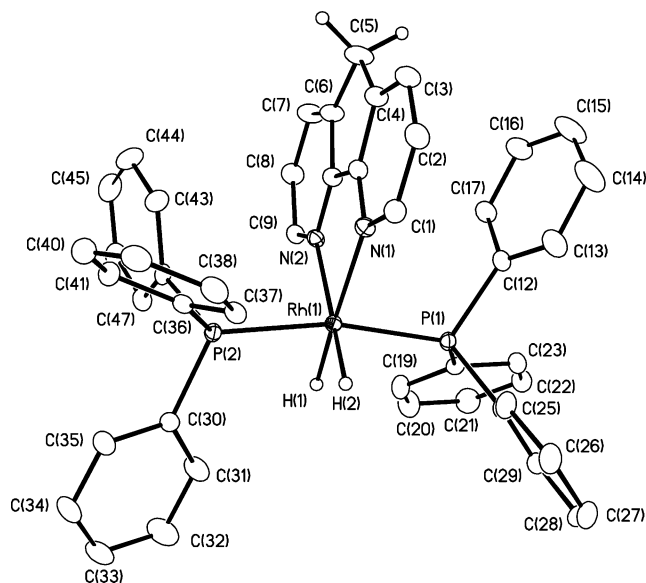


Figure 4. Crystal structure of the Rh-containing cation of **4** with thermal ellipsoids plotted at the 30% probability level. The OTf^- counterion and most of the hydrogen atoms have been omitted for clarity.

Conclusions

A series of novel Rh complexes of L^- and LH ligands have been prepared and fully characterized. The Rh compounds $[\text{Rh}(\text{H})_2(\text{LH})(\text{PPh}_3)_2]\text{Cl}$ (**2**) and $[\text{Rh}(\text{H})_2\text{L}(\text{PPh}_3)_2]$ (**3**) can interconvert cleanly under appropriate conditions. Thus, NaH converts **2** into **3**, whereas aqueous HCl con-

verts **3** into **2**. The clean conversion of $[\text{RhL}(\text{PPh}_3)_2]$ (**1**) into **3** can be achieved under H_2 . Compound **2** is able to promote olefin hydrogenation reactions. Olefin hydrogenation catalysed by **2** appears to have a different mechanism compared with that catalysed by $[\text{Rh}(\text{cod})\text{L}]$. Unlike in Wilkinson's catalyst, in which the chloride is a spectator ligand, the chloride counterion in **2** seems to play a role in olefin hydrogenation processes, as evidenced by the inactivity of $[\text{Rh}(\text{H})_2(\text{LH})(\text{PPh}_3)_2]\text{OTf}$ (**4**) towards olefin hydrogenation. Exogenous chloride ions slow olefin hydrogenation reactions catalysed by **2**. The role of the chloride counterion in olefin hydrogenation promoted by **2** is yet to be determined. Nevertheless **2** and **4** are the first rhodium complexes of the neutral LH ligand.

Experimental Section

General: All reactions were carried out under argon by using standard Schlenk techniques or in a nitrogen-atmosphere glovebox from MBraun. Unless otherwise stated, all chemicals were purchased from commercial sources and used without further purification. Benzene was heated at reflux and distilled from sodium/benzophenone under argon and stored over activated 4 Å molecular sieves in the glovebox. THF and pentane were purified by using the solvent purification system from Vacuum Atmospheres Company. 4,5-Diazafluorene (LH) was prepared according to a literature procedure.^[14] CD_2Cl_2 and C_6D_6 , purchased from Cambridge Isotope Laboratories, Inc., were degassed prior to use. The NMR spectra were recorded with a Varian 400 spectrometer operating at 400 MHz for ^1H , 162 MHz for ^{31}P and 100 MHz for ^{13}C . Elemental analyses were performed at our Chemistry Department with a PE 2400 C/H/N/S analyser.

Synthesis of $[\text{RhL}(\text{PPh}_3)_2]$ (1**):** A purple solution of NaL prepared in situ from LH (50 mg, 0.3 mmol) and NaH (60% in mineral oil, 20 mg, 0.5 mmol) in THF (3 mL) was added dropwise through a cannula to a solution of $[\text{RhCl}(\text{PPh}_3)_3]$ (0.2 g, 0.3 mmol) in THF (5 mL) with stirring. After stirring the resulting dark-brown solution overnight (≈ 12 h), the solvent was removed under reduced pressure. The residue was dissolved in benzene (2 mL) and filtered through a pad of Celite. The filtrate was dried under vacuum to afford a dark-green solid of **1** (0.18 g, 76%). Crystals suitable for X-ray crystallographic analysis were obtained by the slow diffusion of hexanes in a concentrated solution of **1** in benzene. ^1H NMR (C_6D_6 , 400 MHz): $\delta = 7.65\text{--}7.59$ (m, 14 H), 6.64 (d, $J = 4$ Hz, 2 H), 6.58 (t, $J = 7$ Hz, 6 H), 6.53 (s, 1 H), 6.48 (t, $J = 7$ Hz, 12 H), 6.21 (dd, $J_1 = 4$, $J_2 = 9$ Hz, 2 H) ppm. ^{31}P NMR (C_6D_6 , 162 MHz): $\delta = 52.11$ (d, $^1J_{\text{Rh-P}} = 187$ Hz) ppm. ^{13}C NMR (C_6D_6 , 100 MHz): $\delta = 135.04$ (t, $J = 6$ Hz), 134.75, 129.14, 128.16, 127.98, 127.74, 127.64, 127.55, 127.20, 126.51 ppm. $\text{C}_{47}\text{H}_{37}\text{N}_2\text{P}_2\text{Rh}$ (794.68): calcd. C 71.04, H 4.69, N 3.53; found C 70.98, H 4.53, N 3.71.

Synthesis of $[\text{Rh}(\text{H})_2(\text{LH})(\text{PPh}_3)_2]\text{Cl}$ (2**):** A pale-yellow solution of LH (50 mg, 0.3 mmol) in THF (3 mL) was added to an orange solution of $[\text{RhCl}(\text{PPh}_3)_3]$ (0.2 g, 0.3 mmol) in THF (5 mL) with stirring under argon. The flask was then submerged in liquid nitrogen, evacuated and charged with H_2 , leading to the formation of a large amount of a pale-pink precipitate. The mixture was further stirred for 1 h. The precipitate was collected by filtration, washed with THF (10 mL) and dried under vacuum to yield a pale-pink solid of **2** (0.25 g, $>99\%$). Crystals suitable for X-ray crystallographic analysis were obtained from the slow diffusion of hexanes in a concentrated solution of **2** in CH_2Cl_2 . ^1H NMR (CD_2Cl_2 ,

400 MHz): $\delta = 7.89$ (d, $J = 5$ Hz, 2 H), 7.83 (d, $J = 8$ Hz, 2 H), 7.37 (t, $J = 6$ Hz, 12 H), 7.33 (t, $J = 8$ Hz, 6 H), 7.21 (t, $J = 8$ Hz, 12 H), 7.03 (dd, $J_1 = 5$, $J_2 = 8$ Hz, 2 H), 3.83 (s, 2 H), -16.82 (dt, $^1J_{\text{Rh-H}} = 18$, $^2J_{\text{P-H}} = 13$ Hz, 2 H) ppm. ^{31}P NMR (CD_2Cl_2 , 162 MHz): $\delta = 48.62$ (dt, $^1J_{\text{Rh-P}} = 116$, $^2J_{\text{P-H}} = 11$ Hz) ppm. ^{13}C NMR (CD_2Cl_2 , 100 MHz): $\delta = 160.24$, 150.23, 136.69, 134.34, 133.29 (t, $J = 6$ Hz), 130.49 (t, $J = 22$ Hz), 130.45, 128.48 (t, $J = 5$ Hz), 128.40, 35.82 ppm. $\text{C}_{47}\text{H}_{40}\text{ClN}_2\text{P}_2\text{Rh}\cdot\frac{1}{8}\text{CH}_2\text{Cl}_2$ (843.77): calcd. C 67.08, H 4.81, N 3.32; found C 67.23, H 4.72, N 3.41.

Synthesis of [Rh(H)₂L(PPh₃)₂] (3): NaH (60% in mineral oil, 20 mg, 0.5 mmol) was added to a suspension of **2** (0.25 g, 0.3 mmol) in THF (4 mL). The mixture was stirred for 1 d to afford a dark-blue solution, which was then filtered through a pad of Celite to remove NaCl. The filtrate was dried under vacuum to afford a red solid of **3** (0.23 g, 99%). Crystals suitable for X-ray crystallographic analysis were obtained by the slow diffusion of hexanes in a concentrated solution of **3** in benzene. ^1H NMR (C_6D_6 , 400 MHz): $\delta = 7.47$ (d, $J = 8$ Hz, 2 H), 7.15–7.09 (m, 14 H), 6.59–6.52 (m, 18 H), 6.29 (s, 1 H), 6.22 (dd, $J_1 = 5$, $J_2 = 8$ Hz, 2 H), -16.49 (dt, $^1J_{\text{Rh-H}} = 17$, $^2J_{\text{P-H}} = 15$ Hz, 2 H) ppm. ^{31}P NMR (C_6D_6 , 162 MHz): $\delta = 50.19$ (dt, $^1J_{\text{Rh-P}} = 118$, $^2J_{\text{P-H}} = 10$ Hz) ppm. ^{13}C NMR (C_6D_6 , 100 MHz): $\delta = 135.32$, 133.72 (t, $J = 6$ Hz), 129.30, 128.40, 127.98, 127.96, 127.74, 127.68, 127.62, 124.57 ppm. $\text{C}_{47}\text{H}_{39}\text{N}_2\text{P}_2\text{Rh}$ (796.69): calcd. C 70.86, H 4.93, N 3.52; found C 70.50, H 4.94, N 3.45.

Synthesis of [Rh(H)₂(LH)(PPh₃)₂]OTf (4): Compound **2** (42 mg, 0.05 mmol) and AgOTf (13 mg, 0.05 mmol) were stirred in CH_2Cl_2 (3 mL) overnight and filtered to remove the precipitate. The filtrate was dried under vacuum to afford **4** as an off-white solid (40 mg, 84%). Crystals suitable for X-ray crystallographic analysis were obtained by the slow diffusion of pentane into a concentrated solution of **4** in CH_2Cl_2 . ^1H NMR (CD_3OD , 400 MHz): $\delta = 8.06$ (d, $J = 5$ Hz, 2 H), 7.79 (d, $J = 8$ Hz, 2 H), 7.40–7.33 (m, 12 H), 7.31 (t, $J = 7$ Hz, 6 H), 7.22 (t, $J = 7$ Hz, 12 H), 7.07 (dd, $J_1 = 5$, $J_2 = 8$ Hz, 2 H), 3.80 (s, 2 H), -16.75 (dt, $^1J_{\text{Rh-H}} = 18$, $^2J_{\text{P-H}} = 13$ Hz, 2 H) ppm. ^{31}P NMR (CD_3OD , 162 MHz): $\delta = 48.28$ (dt, $^1J_{\text{Rh-P}} = 116$, $^2J_{\text{P-H}} = 11$ Hz) ppm. ^{19}F NMR (CD_3OD): $\delta = -80.55$ (s) ppm. ^{13}C NMR (CD_2Cl_2 , 100 MHz): $\delta = 160.36$, 150.57, 136.94, 134.02,

133.18 (t, $J = 7$ Hz), 132.58 (t, $J = 18$ Hz), 130.20, 128.27 (t, $J = 5$ Hz), 125.23, 124.84 (q, $J = 316$ Hz), 35.01 ppm. $\text{C}_{48}\text{H}_{40}\text{N}_2\text{O}_3\text{F}_3\text{P}_2\text{SRh}\cdot 0.5\text{CH}_2\text{Cl}_2$ (989.23): calcd. C 58.89, H 4.18, N 2.83; found C 59.20, H 4.27, N 2.67.

Olefin Hydrogenation Promoted by 2: At ambient temperature a glass vessel was charged with 1 atm of H_2 , 3 mg of **2** (0.0035 mmol), an olefin substrate (7 mmol) and MeOH (to reach a total volume of 1 mL). The progress of the reaction was monitored by ^1H NMR spectroscopy (compared with the spectra reported in the literature).

X-ray Diffraction Analysis: All crystals were mounted on the tip of a MiTeGen MicroMount. The single-crystal X-ray diffraction data for **1–3** were collected with a Nonius-Kappa CCD diffractometer, whereas the data for **4** were collected with a Bruker Kappa APEX II diffractometer. In all cases, the collection conditions were as follows: Mo- K_α radiation ($\lambda = 0.71073$ Å), 50 kV, 30 mA and 150 K controlled by an Oxford Cryostream 700 series low-temperature

Table 3. Selected bond lengths [Å] and angles [°].

1			
Rh(1)–N(2)	2.196(2)	N(2)–Rh(1)–P(2)	94.66(6)
Rh(1)–N(1)	2.199(2)	N(1)–Rh(1)–P(2)	170.54(7)
Rh(1)–P(2)	2.2217(7)	N(2)–Rh(1)–P(1)	165.47(7)
Rh(1)–P(1)	2.2357(7)	N(1)–Rh(1)–P(1)	91.42(6)
C(4)–C(5)	1.412(5)	P(2)–Rh(1)–P(1)	93.67(3)
C(5)–C(6)	1.419(4)	C(4)–C(5)–C(6)	107.7(3)
N(2)–Rh(1)–N(1)	82.10(9)		
2			
Rh(1)–H(2)	1.53(7)	H(1)–Rh(1)–N(1)	95(2)
Rh(1)–H(1)	1.60(7)	N(2)–Rh(1)–N(1)	80.53(12)
Rh(1)–N(2)	2.223(3)	H(2)–Rh(1)–P(1)	87.13(15)
Rh(1)–N(1)	2.234(3)	H(1)–Rh(1)–P(1)	86.16(11)
Rh(1)–P(1)	2.2994(7)	N(2)–Rh(1)–P(1)	94.060(19)
Rh(1)–P(1A)	2.2994(7)	N(1)–Rh(1)–P(1)	93.002(19)
C(4)–C(5)	1.513(6)	H(2)–Rh(1)–P(1A)	87.13(15)
C(5)–C(6)	1.532(6)	H(1)–Rh(1)–P(1A)	86.16(10)
H(2)–Rh(1)–H(1)	88(3)	N(2)–Rh(1)–P(1A)	94.060(19)
H(2)–Rh(1)–N(2)	97(2)	N(1)–Rh(1)–P(1A)	93.002(19)
H(1)–Rh(1)–N(2)	175(2)	P(1)–Rh(1)–P(1A)	170.60(4)
H(2)–Rh(1)–N(1)	178(2)	C(4)–C(5)–C(6)	101.8(3)
3			
Rh(1)–H(1)	1.47(4)	H(1)–Rh(1)–N(1)	176.6(15)
Rh(1)–H(2)	1.48(6)	N(2)–Rh(1)–N(1)	81.49(16)
Rh(1)–N(2)	2.192(4)	N(2)–Rh(1)–P(2)	99.83(11)
Rh(1)–N(1)	2.235(4)	N(1)–Rh(1)–P(2)	94.65(11)
Rh(1)–P(2)	2.2892(13)	N(2)–Rh(1)–P(1)	92.80(11)
Rh(1)–P(1)	2.2967(13)	N(1)–Rh(1)–P(1)	98.68(11)
C(4)–C(5)	1.403(8)	P(2)–Rh(1)–P(1)	162.85(5)
C(5)–C(6)	1.426(8)	H(2)–Rh(1)–P(2)	82(2)
H(2)–Rh(1)–H(1)	81(3)	H(1)–Rh(1)–P(2)	83.3(15)
H(2)–Rh(1)–N(2)	177(2)	H(2)–Rh(1)–P(1)	85(2)
H(1)–Rh(1)–N(2)	96.2(15)	H(1)–Rh(1)–P(1)	83.8(15)
H(2)–Rh(1)–N(1)	101(2)	C(4)–C(5)–C(6)	108.6(5)
4			
Rh(1)–N(1)	2.207(2)	N(2)–Rh(1)–P(1)	91.61(6)
Rh(1)–N(2)	2.232(2)	P(2)–Rh(1)–P(1)	169.71(2)
Rh(1)–P(2)	2.2910(7)	N(1)–Rh(1)–H(1)	179.0(13)
Rh(1)–P(1)	2.3175(7)	N(2)–Rh(1)–H(1)	99.1(12)
Rh(1)–H(1)	1.47(3)	P(2)–Rh(1)–H(1)	85.2(12)
Rh(1)–H(2)	1.45(3)	P(1)–Rh(1)–H(1)	86.7(12)
C(4)–C(5)	1.516(4)	N(1)–Rh(1)–H(2)	97.5(13)
C(5)–C(6)	1.518(4)	N(2)–Rh(1)–H(2)	177.6(13)
N(1)–Rh(1)–N(2)	80.52(8)	P(2)–Rh(1)–H(2)	85.6(13)
N(1)–Rh(1)–P(2)	95.83(6)	P(1)–Rh(1)–H(2)	87.1(13)
N(2)–Rh(1)–P(2)	95.94(6)	H(1)–Rh(1)–H(2)	82.8(18)
N(1)–Rh(1)–P(1)	92.29(6)	C(4)–C(5)–C(6)	103.1(2)

Table 2. Crystallographic data.

	1 • C_6H_6	2 • $2\text{CH}_2\text{Cl}_2$	3 • C_6H_6	4
Formula	$\text{C}_{53}\text{H}_{43}\text{N}_2\text{P}_2\text{Rh}$	$\text{C}_{49}\text{H}_{44}\text{Cl}_4\text{N}_2\text{P}_2\text{Rh}$	$\text{C}_{53}\text{H}_{43}\text{N}_2\text{P}_2\text{Rh}$	$\text{C}_{48}\text{H}_{40}\text{F}_3\text{N}_2\text{O}_3\text{P}_2\text{SRh}$
<i>FW</i>	872.74	1002.96	874.76	946.73
<i>T</i> [K]	150(2)	150(2)	150(2)	150(2)
space group	<i>Pt</i>	<i>Pbcm</i>	<i>P2_1/c</i>	<i>Pt</i>
<i>a</i> [Å]	12.8501(5)	10.7680(2)	22.1158(4)	11.1606(2)
<i>b</i> [Å]	13.1764(7)	18.1569(3)	20.1085(3)	13.7726(4)
<i>c</i> [Å]	14.4450(5)	23.2429(5)	19.3214(3)	17.2066(6)
α [deg]	72.187(2)	90	90	92.469(1)
β [deg]	77.447(3)	90	100.721(1)	96.154(1)
γ [deg]	64.959(2)	90	90	113.864(1)
<i>V</i> [Å ³]	2098.70(16)	4544.30(15)	8442.5(2)	2393.89(12)
<i>Z</i>	2	4	8	2
<i>D_c</i> [g•cm ⁻³]	1.381	1.466	1.376	1.313
μ [mm ⁻¹]	0.523	0.777	0.520	0.519
no. of refln collected	19791	29452	44891	39892
no. of indep refln	9481	5307	16521	10977
GOF on <i>F</i> ²	1.046	1.082	1.029	1.082
<i>R</i> [<i>I</i> > 2 σ (<i>I</i>)]	<i>R</i> ₁ = 0.0433 <i>wR</i> ₂ = 0.0989	<i>R</i> ₁ = 0.0415 <i>wR</i> ₂ = 0.0938	<i>R</i> ₁ = 0.0580 <i>wR</i> ₂ = 0.1383	<i>R</i> ₁ = 0.0423 <i>wR</i> ₂ = 0.1097
<i>R</i> (all data)	<i>R</i> ₁ = 0.0599 <i>wR</i> ₂ = 0.1097	<i>R</i> ₁ = 0.0687 <i>wR</i> ₂ = 0.1077	<i>R</i> ₁ = 0.1245 <i>wR</i> ₂ = 0.1826	<i>R</i> ₁ = 0.0494 <i>wR</i> ₂ = 0.1131

system. The diffraction data for **1–3** were processed with the DENZO-SMN^[15] software package, whereas the data for **4** were processed with the Bruker APEX2 software package (V2008.3).^[16] All structures were solved by direct methods and refined with SHELXTL (V6.10).^[17] All non-hydrogen atoms were refined anisotropically except for those involved in disordering. The positions of the hydrogen atoms were either calculated or directly located from a difference Fourier map and their contributions were included in the structure factor calculations. Compound **1** co-crystallized with benzene (one benzene molecule per molecule of **1**) in the triclinic space group $P\bar{1}$. Compound **2** co-crystallized with CH₂Cl₂ (two CH₂Cl₂ molecules per molecule of **2**) in the orthorhombic space group $Pbcm$. Compound **3** co-crystallized with benzene (one benzene molecule per molecule of **3**) in the monoclinic space group $P2_1/c$ with two independent molecules per asymmetric unit. Compound **4** crystallized in the triclinic space group $P\bar{1}$. The co-crystallized solvent molecule was badly disordered and therefore was removed by using the SQUEEZE routine of the PLATON program.^[18] Although the identity of the solvent could not be confirmed by crystallography, the elemental analysis results suggest the presence of CH₂Cl₂ in the crystal lattice even after vacuum drying. The contribution of the removed solvent was not included in the final formula and density calculations. The crystallographic data for **1–4** are summarized in Table 2 and selected bond lengths and angles are listed in Table 3.

CCDC-712062 (for **1**·C₆H₆), 712063 (for **2**·2CH₂Cl₂), 712064 (for **3**·C₆H₆) and CCDC-712065 (for **4**) contain the supplementary crystallographic data for this paper. These data can be obtained free of charge from the Cambridge Crystallographic Data Centre via www.ccdc.cam.ac.uk/data_request/cif.

Acknowledgments

This research was supported by grants to D. S. from the Natural Science and Engineering Research Council (NSERC) of Canada, the Canadian Foundation for Innovation, the Ontario Research Fund (ORF) and the University of Toronto (Connaught Foundation).

- [1] a) K. Kloc, J. Mlochowski, Z. Szule, *J. Prakt. Chem.* **1977**, *319*, 959–967; b) K. Kloc, Z. Szule, J. Mlochowski, *Heterocycles* **1978**, *9*, 849–852; c) K. Ono, K. Saito, *Heterocycles* **2008**, *75*, 2381–2413.
- [2] a) L. J. Henderson Jr., F. R. Fronczek, W. R. Cherry, *J. Am. Chem. Soc.* **1984**, *106*, 5876–5879; b) W. M. Wacholtz, R. A. Auerbach, R. H. Schmehl, M. Ollino, W. R. Cherry, *Inorg. Chem.* **1985**, *24*, 1758–1760; c) R. P. Thummel, F. Lefoulon, J. D. Korp, *Inorg. Chem.* **1987**, *26*, 2370–2376; d) T. C. Streckas, H. D. Gafney, S. A. Tysoe, R. P. Thummel, F. Lefoulon, *Inorg. Chem.* **1989**, *28*, 2964–2967; e) T. C. Streckas, H. D. Gafney, S. A. Tysoe, R. P. Thummel, F. Lefoulon, *Inorg. Chem.* **1989**, *28*, 4306; f) K. Maruszewski, J. R. Kincaid, *Inorg. Chem.* **1995**, *34*, 2002–2006; g) M. Sykora, J. R. Kincaid, *Inorg. Chem.* **1995**, *34*, 5852–5856.
- [3] a) D. E. Marx, A. J. Lees, *Inorg. Chem.* **1987**, *26*, 620–622; b) A. Baysal, J. A. Connor, J. D. Wallis, *J. Coord. Chem.* **2001**, *53*, 347–354; c) R. A. Klein, R. van Belzen, K. Vrieze, C. J. Elsevier, R. P. Thummel, J. Fraanje, K. Goubitz, *Collect. Czech. Chem. Commun.* **1997**, *62*, 238–256.
- [4] H. Jiang, E. Stepowska, D. Song, *Dalton Trans.* **2008**, 5879–5881.
- [5] H. Jiang, D. Song, *Organometallics* **2008**, *27*, 3587–3592.
- [6] T. E. Bitterwolf, *Inorg. Chim. Acta* **1986**, *122*, 175–184.
- [7] Á. Álvarez, R. Macías, M. J. Fabra, M. L. Martín, F. J. Lahoz, L. A. Oro, *Inorg. Chem.* **2007**, *46*, 6811–6826.
- [8] K. Nikki, H. Inakura, Wu-Le, N. Suzuki, T. Endo, *J. Chem. Soc. Perkin Trans. 2* **2001**, 2370–2373.
- [9] B. P. S. Chauhan, J. S. Rathore, T. Bando, *J. Am. Chem. Soc.* **2004**, *126*, 8493–8500.
- [10] G. M. Rubottom, E. J. Evain, *Tetrahedron* **1990**, *46*, 5055–5064.
- [11] C. Gingreau, J.-C. Galin, *Polymer* **1994**, *35*, 4669–4677.
- [12] M. E. Rosen, S. P. Rucker, C. Schmidt, A. Pines, *J. Phys. Chem.* **1993**, *97*, 3858–3866.
- [13] A. C. Buchanan, A. S. Dworkin, G. P. Smith, *J. Am. Chem. Soc.* **1983**, *105*, 2843–2850.
- [14] M. J. Plater, S. Kemp, E. Lattmann, *J. Chem. Soc. Perkin Trans. 1* **2000**, 971–979.
- [15] Z. Otwinowski, W. Minor in *Methods in Enzymology, Macromolecular Crystallography, Part A* (Eds.: C. W. Carter, R. M. Sweet), Academic Press, London, **1997**, vol. 276, pp. 307–326.
- [16] *Apex 2 software package*, Bruker AXS Inc., **2008**.
- [17] G. M. Sheldrick, *Acta Crystallogr., Sect. A* **2008**, *64*, 112–122.
- [18] A. L. Spek, *J. Appl. Crystallogr.* **2003**, *36*, 7–13.

Received: December 9, 2008

Published Online: February 17, 2009